Scientific Research Publishing

International Journal of Astronomy and Astrophysics, 2023, 13, 25-38
https://www.scirp.org/journal/ijaa
ISSN Online: 2161-4725
ISSN Print: 2161-4717

A Study of Warm Dark Matter, the Missing Satellites Problem, and the UV Luminosity Cut-Off

Bruce Hoeneisen

Universidad San Francisco de Quito, Quito, Ecuador
Email: bhoeneisen@usfq.edu.ec

How to cite this paper: Hoeneisen, B. (2023) A Study of Warm Dark Matter, the Missing Satellites Problem, and the UV Luminosity Cut-Off. *International Journal of Astronomy and Astrophysics*, **13**, 25-38.
https://doi.org/10.4236/ijaa.2023.131002

Received: January 11, 2023
Accepted: March 20, 2023
Published: March 23, 2023

Abstract

In the warm dark matter scenario, the Press-Schechter formalism is valid only for galaxy masses greater than the "velocity dispersion cut-off". In this work we extend the predictions to masses below the velocity dispersion cut-off, and thereby address the "Missing Satellites Problem" of the cold dark matter ΛCDM scenario, and the rest-frame ultra-violet luminosity cut-off required to not exceed the measured reionization optical depth. For warm dark matter we find agreement between predictions and observations of these two phenomena. As a by-product, we obtain the empirical Tully-Fisher relation from first principles.

Keywords

Cosmology: Dark Matter, Galaxies: Statistics

1. Introduction

Two apparent problems with the cold dark matter ΛCDM cosmology are the "Missing Satellites Problem", and the need of a rest-frame ultra-violet (UV) luminosity cut-off. The "Missing Satellites Problem" is the reduced number of observed Local Group satellites compared to the number obtained in ΛCDM simulations [1]. A UV luminosity cut-off is needed to not exceed the reionization optical depth $\tau = 0.054 \pm 0.007$ measured by the Planck collaboration [2] [3] [4] [5]. In the present study we consider warm dark matter as a possible solution to both problems.

The Press-Schechter formalism, when applied to warm dark matter, includes the free-streaming cut-off, but not the "velocity dispersion cut-off", and is therefore only valid for total (dark matter plus baryon) linear perturbation masses M

greater than the velocity dispersion cut-off mass M_{vd} (to be explained below). The purpose of the present study is to extend the Press-Schechter prediction to $M < M_{\mathrm{vd}}$, and compare this extension with the "Missing Satellites Problem", and with the needed UV luminosity cut-off.

We continue the study of warm dark matter presented in [6]. Our point of departure is **Figure 1** of [6]. Here we reproduce the panel corresponding to redshift $z = 6$ in **Figure 1** (with one change: instead of the Gaussian window function in [6], in the present article we use the sharp-k window function throughout, with mass parameter $c = 1.555$ as explained in [6]). **Figure 1** compares distributions, *i.e.* numbers of galaxies per decade (dex) and per Mpc^3, of galaxy linear total (dark matter plus baryon) perturbation masses M, stellar masses M_*, and rest-frame ultra-violet (UV) luminosities νL_{UV}, with the Press-Schechter prediction [7], and its Sheth-Tormen ellipsoidal collapse extensions with parameter $\nu \equiv 1.686/\sigma$ (not to be confused with the frequency above) and 0.84ν [8] [9]. The data on M_* is obtained from [10] [11] [12] [13]. The data on νL_{UV}, where ν is the frequency corresponding to wavelength 1550 Å, is obtained from [4] [14] [15] [16]. The UV luminosities have been corrected for dust extinction as described in [4] [17]. The predictions depend on the warm dark matter free-streaming comoving cut-off wavenumber $k_{\mathrm{fs}}(t_{\mathrm{eq}})$, and the comparisons of predictions with

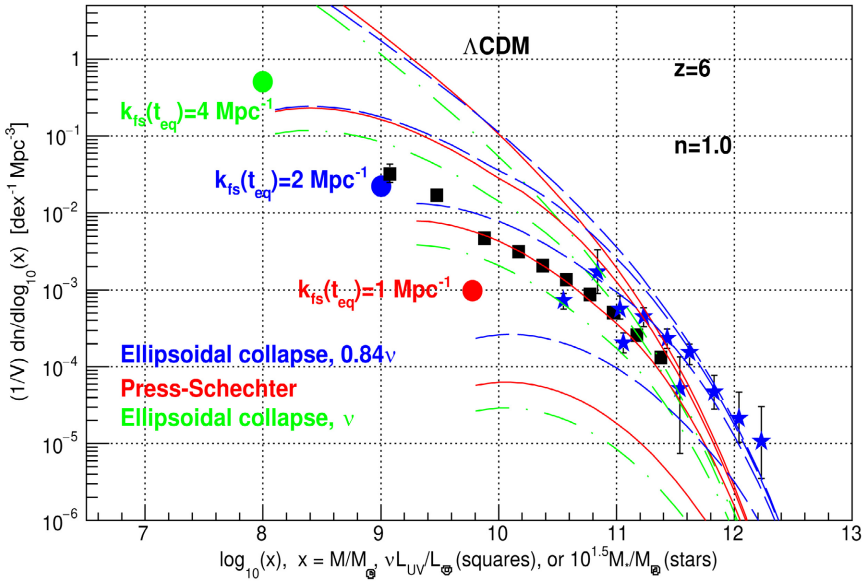

Figure 1. Shown are distributions of x, where x is the observed galaxy stellar mass $M_*/M_\odot$ times $10^{1.5}$ (stars) [10] [11] [12] [13], or the observed galaxy UV luminosity $\nu L_{\mathrm{UV}}/L_\odot$ (squares) [4] [14] [15] [16] (corrected for dust extinction [4] [17]), or the predicted linear total (dark matter plus baryon) mass $M/M_\odot$ (lines), at redshift $z = 6$. The Press-Schechter prediction, and its Sheth-Tormen ellipsoidal collapse extensions, correspond, from top to bottom, to the warm dark matter free-streaming cut-off wavenumbers $k_{\mathrm{fs}}(t_{\mathrm{eq}}) = 1000, 4, 2$ and 1 Mpc^{-1}. The round red, blue and green dots indicate the velocity dispersion cut-offs M_{vd} of the predictions [18] at $k_{\mathrm{fs}}(t_{\mathrm{eq}}) = 1, 2$ and 4 Mpc^{-1}, respectively. Presenting three predictions illustrates the uncertainty of the predictions.

data provide a measurement of $k_{\mathrm{fs}}\left(t_{\mathrm{eq}}\right)$, see [6] for full details. In **Figure 1** the predictions extend down to the velocity dispersion cut-offs indicated by red, blue and green dots [6] [18]. The purpose of the present study is to extend the predictions to smaller M_* and νL_{UV}, and thereby address the "Missing Satellites Problem", and the UV luminosity cut-off, respectively.

2. Velocity Dispersion and Free-Streaming

To obtain a self-contained article, we need to define the warm dark matter adiabatic invariant $v_{h\mathrm{rms}}(1)$, and the free-streaming cut-off factor $\tau^2(k)$. We consider non-relativistic warm dark matter to be a clasical (non-degenerate) gas of particles, as justified in [19] [20]. Let $v_{h\mathrm{rms}}(a)$ be the root-mean-square velocity of non-relativistic warm dark matter particles in the early universe at expansion parameter a. As the universe expands it cools, so $v_{h\mathrm{rms}}(a)$ decreases in proportion to a^{-1} (if dark matter collisions, if any, do not excite particle internal degrees of freedom [21]). Therefore,

$$v_{h\mathrm{rms}}(1) = v_{h\mathrm{rms}}(a)\,a = v_{h\mathrm{rms}}(a)\left[\frac{\Omega_c \rho_{\mathrm{crit}}}{\rho_h(a)}\right]^{1/3}, \tag{1}$$

is an adiabatic invariant. $\rho_h(a) = \Omega_c \rho_{\mathrm{crit}}/a^3$ is the dark matter density. The warm dark matter velocity dispersion causes free-streaming of dark matter particles in and out of density minimums and maximums, and so attenuates the power spectrum of relative density perturbations $\left(\rho(\boldsymbol{x}) - \overline{\rho}\right)/\overline{\rho}$ of the cold dark matter ΛCDM cosmology by a factor $\tau^2(k)$. k is the comoving wavenumber of relative density perturbations. At the time t_{eq} of equal radiation and matter densities, $\tau^2(k)$ has the approximate form [22]

$$\tau^2(k) \approx \exp\left[-k^2/k_{\mathrm{fs}}^2\left(t_{\mathrm{eq}}\right)\right], \tag{2}$$

where the comoving cut-off wavenumber, due to free-streaming, is [22]

$$k_{\mathrm{fs}}\left(t_{\mathrm{eq}}\right) = \frac{1.455}{\sqrt{2}}\sqrt{\frac{4\pi G \overline{\rho}_h(1)\, a_{\mathrm{eq}}}{v_{h\mathrm{rms}}(1)^2}}. \tag{3}$$

After t_{eq}, the Jeans mass decreases as $a^{-3/2}$, so $\tau^2(k)$ develops a non-linear regenerated "tail" when the relative density perturbations approach unity [23]. We will take $\tau^2(k)$, at the time of galaxy formation, to have the form

$$\tau^2(k) = \begin{cases} \exp\left(-\dfrac{k^2}{k_{\mathrm{fs}}^2\left(t_{\mathrm{eq}}\right)}\right) & \text{if } k < k_{\mathrm{fs}}\left(t_{\mathrm{eq}}\right), \\ \exp\left(-\dfrac{k^n}{k_{\mathrm{fs}}^n\left(t_{\mathrm{eq}}\right)}\right) & \text{if } k \geq k_{\mathrm{fs}}\left(t_{\mathrm{eq}}\right). \end{cases} \tag{4}$$

The parameter n allows a study of the effect of the non-linear regenerated tail. If $n = 2$, there is no regenerated tail. Agreement between the data and predictions, down to the velocity dispersion cut-off dots in **Figure 1**, is obtained with n in the approximate range 1.1 to 0.2 [6].

A comment: In (4) we should have written $k_{\mathrm{fs}}\left(t_{\mathrm{gal}}\right)$ instead of $k_{\mathrm{fs}}\left(t_{\mathrm{eq}}\right)$, where t_{gal} is the time of galaxy formation. However, the measurement $k_{\mathrm{fs}}\left(t_{\mathrm{gal}}\right)=2.0^{+0.8}_{-0.5}\ \mathrm{Mpc}^{-1}$, with galaxy UV luminosity distributions and galaxy stellar mass distributions [6], is in agreement with the measurement of $k_{\mathrm{fs}}\left(t_{\mathrm{eq}}\right)=1.90\pm0.32\ \mathrm{Mpc}^{-1}$ with dwarf galaxy rotation curves (from the measurement of the adiabatic invariant $v_{h\mathrm{rms}}(1)=0.406\pm0.069\ \mathrm{km/s}$ in [21], and Equation (3)). So we do not distinguish $k_{\mathrm{fs}}\left(t_{\mathrm{gal}}\right)$ from $k_{\mathrm{fs}}\left(t_{\mathrm{eq}}\right)$ (until observations require otherwise).

Let us now consider the velocity dispersion cut-off. In the ΛCDM scenario, when a spherically symmetric relative density perturbation $\left(\rho(\boldsymbol{x})-\overline{\rho}\right)/\overline{\rho}$ reaches 1.686 in the linear approximation, the exact solution diverges, and a galaxy forms. This is the basis of the Press-Schechter formalism. The same is true in the warm dark matter scenario if the linear total (dark matter plus baryon) perturbation mass M exceeds the velocity dispersion cut-off M_{vd0}. For $M<M_{\mathrm{vd0}}$, the galaxy formation redshift z is delayed by Δz due to the velocity dispersion. This delay Δz is not included in the Press-Schechter formalism. Δz is obtained by numerical integration of the galaxy formation hydro-dynamical equations, see [18]. The velocity dispersion cut-off mass M_{vd}, indicated by the dots in **Figure 1**, corresponds, by definition, to $\Delta z=1$. The values of M_{vd} are presented in [6]. For $M>M_{\mathrm{vd0}}=10^{0.67}M_{\mathrm{vd}}$ we take $\Delta z=0$. For $M<M_{\mathrm{vd0}}=10^{0.67}M_{\mathrm{vd}}$ we may approximate $\Delta z\approx 1.5\left[\log_{10}\left(M_{\mathrm{vd}}/M_{\odot}\right)+0.67-\log_{10}\left(M/M_{\odot}\right)\right]$. The values of $\log_{10}\left(M_{\mathrm{vd}}/M_{\odot}\right)$ are summarized in **Table 1**.

3. Extending the Predictions to $M < M_{\mathrm{vd0}}$

The Press-Schechter prediction, and its extensions, are based on the variance $\sigma^2\left(M,z,k_{\mathrm{fs}}\left(t_{\mathrm{eq}}\right),n\right)$ of the linear relative density perturbation $\left(\rho(\boldsymbol{x})-\overline{\rho}\right)/\overline{\rho}$ at the total (dark matter plus baryon) mass scale M [6] [24]. This variance depends on the redshift z of galaxy formation, and on the parameters $k_{\mathrm{fs}}\left(t_{\mathrm{eq}}\right)$ and n of the free-streaming cut-off factor $\tau^2(k)$ of (4). Comparison of predictions and data for $M>M_{\mathrm{vd0}}$ obtain a measurement of $k_{\mathrm{fs}}\left(t_{\mathrm{eq}}\right)$, see **Figure 1**, and [6]. The extension of the predictions to $M<M_{\mathrm{vd0}}$ depends on two cut-offs: the free-streaming cut-off (through the parameters $k_{\mathrm{fs}}\left(t_{\mathrm{eq}}\right)=2.0^{+0.8}_{-0.5}\ \mathrm{Mpc}^{-1}$, that is already fixed by the measurements in [6], and n), and the velocity dispersion cut-off. We illustrate the effect of n in **Figure 2**, without applying the velocity dispersion cut-off yet. The velocity dispersion cut-off is implemented by replacing $\sigma^2\left(M,z,k_{\mathrm{fs}}\left(t_{\mathrm{eq}}\right),n\right)$ by $\sigma^2\left(M,z+\Delta z,k_{\mathrm{fs}}\left(t_{\mathrm{eq}}\right),n\right)$, with Δz obtained from **Table 1**. We illustrate the effect of both n, and the velocity dispersion cut-off, in **Figures 3-5**, for galaxy formation at $z=8,6$, and 4, respectively.

4. The Relation between M and V_{flat}

The linear perturbation total (dark matter plus baryon) mass scale M, of the Press-Schechter formalism, cannot be measured directly. We find that the flat

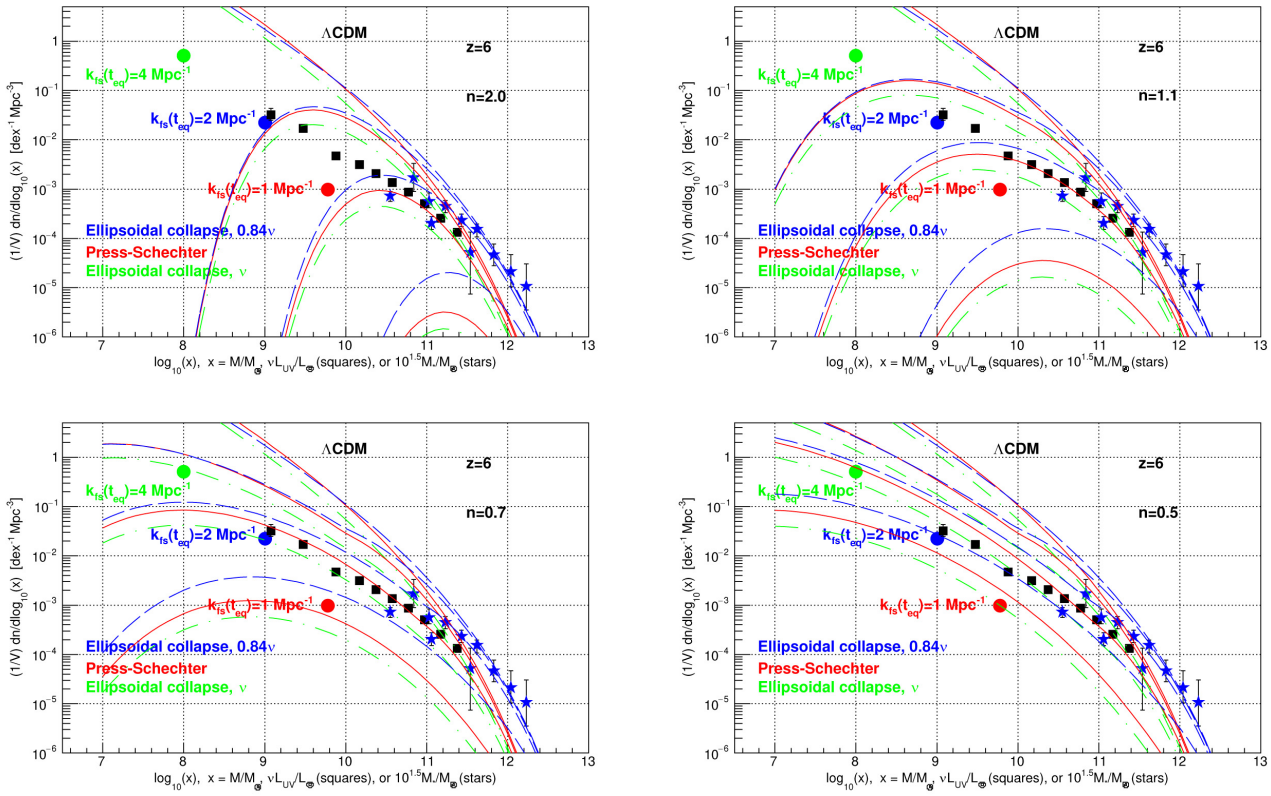

Figure 2. Same as **Figure 1**, *i.e.* $z=6$, but the predictions are extended to $M<M_{\mathrm{vd0}}$ with the free-streaming cut-off with $\tau^2(k)$ with a tail with $n=2.0,1.1,0.7$ or 0.5, *without* the velocity dispersion cut-off.

Table 1. The warm dark matter velocity dispersion delays the galaxy formation redshift z by $\Delta z \approx 1.5\left[\log_{10}\left(M_{\mathrm{vd}}/M_{\odot}\right)+0.67-\log_{10}\left(M/M_{\odot}\right)\right]$ if $M<M_{\mathrm{vd0}}=10^{0.67}M_{\mathrm{vd}}$. The values of $\log_{10}\left(M_{\mathrm{vd}}/M_{\odot}\right)$ are presented as a function of the galaxy formation redshift z, and the adiabatic invariant $v_{h\mathrm{rms}}(1)$. M_{vd} is obtained from numerical integrations of galaxy formation hydro-dynamical equations [18]. Also shown is $k_{\mathrm{fs}}\left(t_{\mathrm{eq}}\right)$ form (3). By definition, at $M=M_{\mathrm{vd}}$ $\Delta z=1.0$.

z	$v_{h\mathrm{rms}}(1)$	$k_{\mathrm{fs}}\left(t_{\mathrm{eq}}\right)$	$\log_{10}\left(M_{\mathrm{vd}}/M_{\odot}\right)$
4	0.75 km/s	1 Mpc^{-1}	9.3
4	0.49 km/s	1.53 Mpc^{-1}	8.5
4	0.37 km/s	2 Mpc^{-1}	8.3
4	0.19 km/s	4 Mpc^{-1}	7.5
6	0.75 km/s	1 Mpc^{-1}	9.8
6	0.49 km/s	1.53 Mpc^{-1}	9.3
6	0.37 km/s	2 Mpc^{-1}	9.0
6	0.19 km/s	4 Mpc^{-1}	8.0
8	0.75 km/s	1 Mpc^{-1}	10.3
8	0.49 km/s	1.53 Mpc^{-1}	9.6
8	0.37 km/s	2 Mpc^{-1}	9.2
8	0.19 km/s	4 Mpc^{-1}	8.2

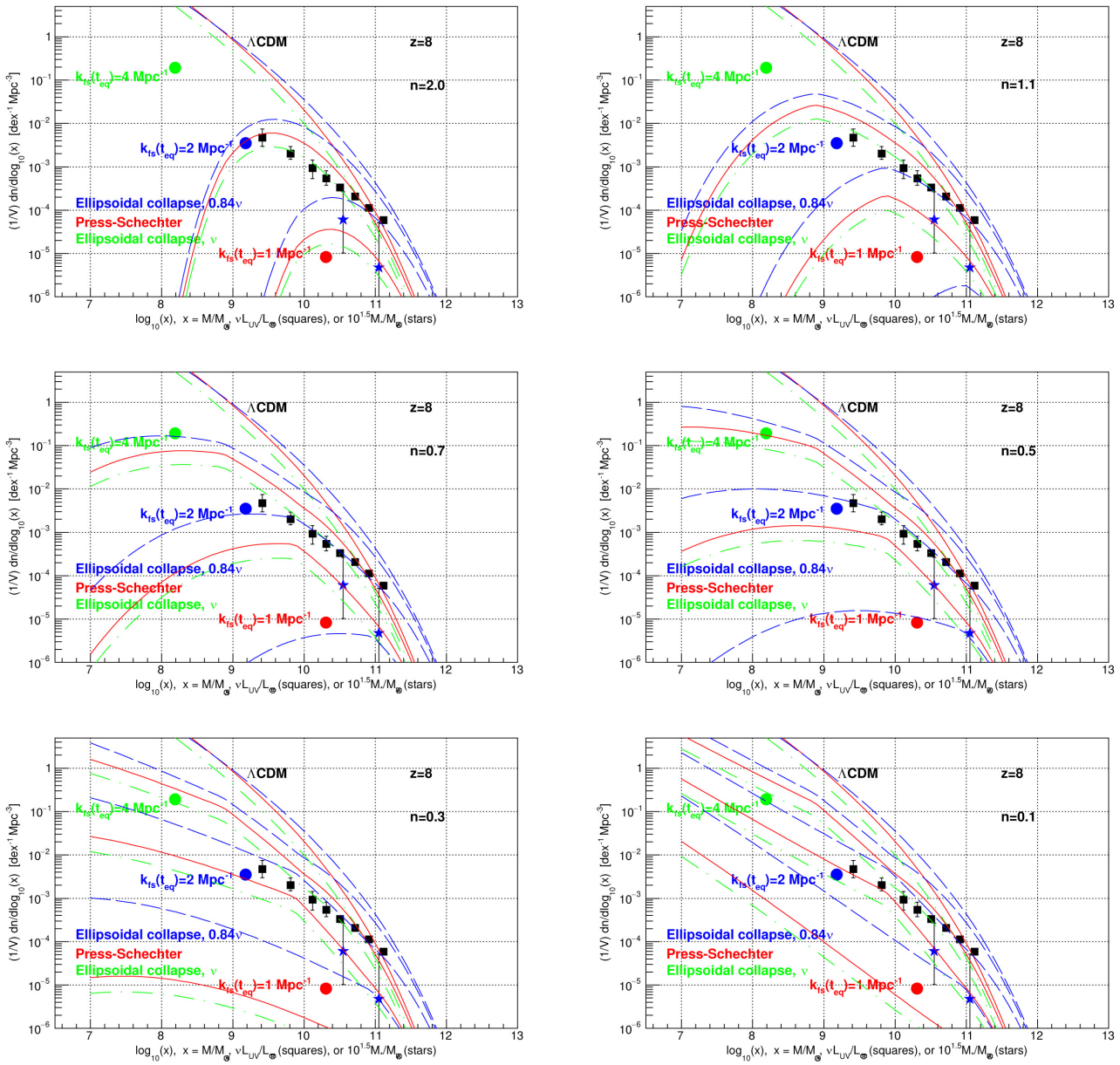

Figure 3. Predictions for $z = 8$, and (from top to bottom) $k_{\mathrm{fs}}(t_{\mathrm{eq}}) = 1000, 4, 2, 1\ \mathrm{Mpc}^{-1}$, are extended to $M < M_{\mathrm{vd0}}$ with the free-streaming cut-off with $\tau^2(k)$ with a tail with $n = 2.0, 1.1, 0.7, 0.5, 0.3$, or 0.1, and with the velocity dispersion cut-off. Agreement between predictions and observations are obtained with $k_{\mathrm{fs}}(t_{\mathrm{eq}}) \approx 2\ \mathrm{Mpc}^{-1}$, and $0.8 \gtrsim n \gtrsim 0.3$.

portion of the rotation velocity of test particles in spiral galaxies, V_{flat}, can be used as an approximate proxy for *M*.

Given *M*, the galaxy formation redshift *z*, and $v_{h\mathrm{rms}}(1)$, it is possible to obtain V_{flat} by numerical integration of the galaxy formation hydro-dynamical equations [18]. Results for $M = 2\times10^{10} M_{\odot}$ are presented in **Table 2**. We note that for galaxy formation at redshift *z* between 6 and 10, and free-streaming cut-off wavenumber $k_{\mathrm{fs}}(t_{\mathrm{eq}})$ between 1 and 1000 Mpc^{-1}, we may approximate

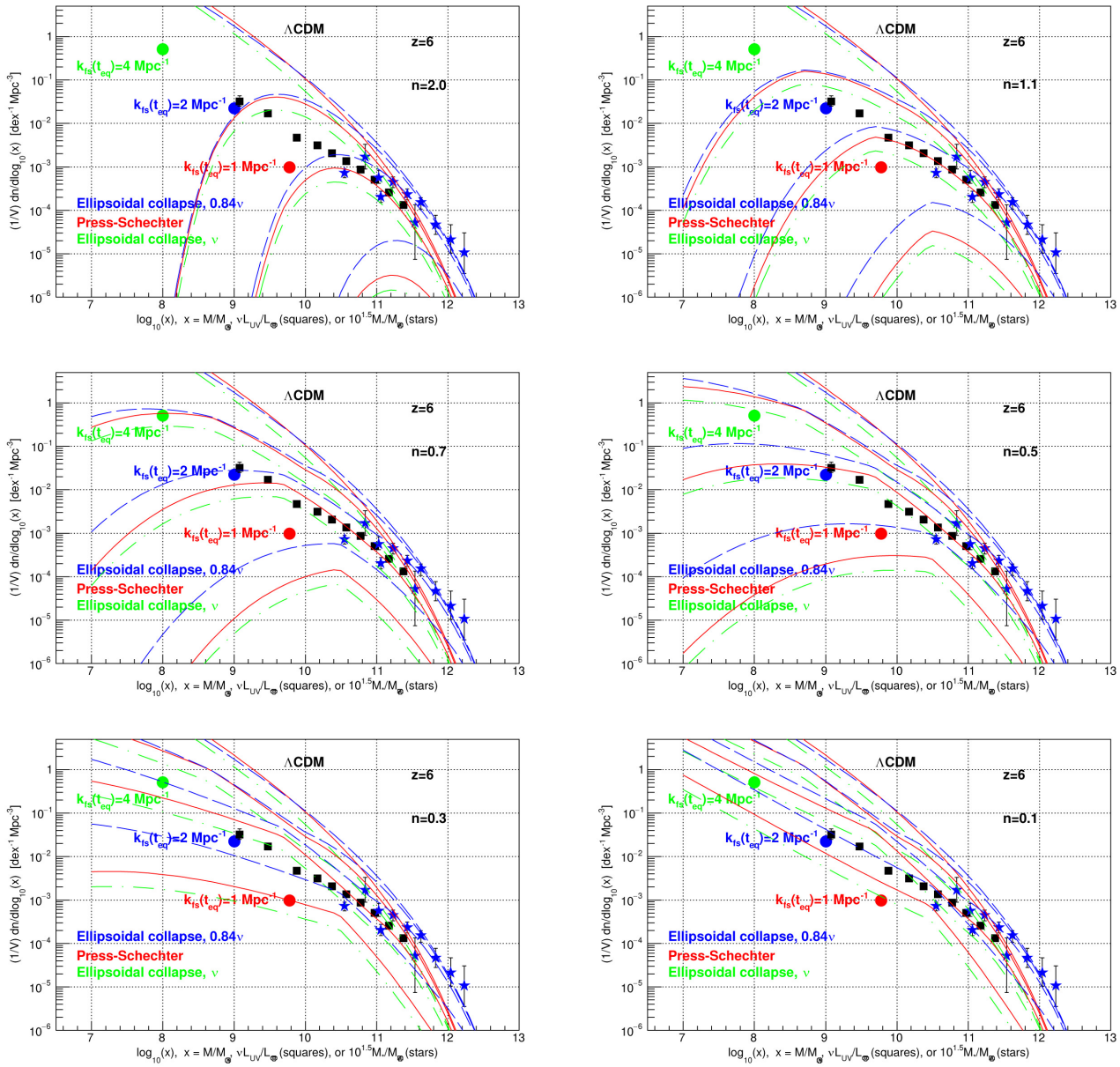

Figure 4. Predictions for $z = 6$, and (from top to bottom) $k_{\mathrm{fs}}(t_{\mathrm{eq}}) = 1000, 4, 2, 1\ \mathrm{Mpc}^{-1}$, are extended to $M < M_{\mathrm{vd0}}$ with the free-streaming cut-off with $\tau^2(k)$ with a tail with $n = 2.0, 1.1, 0.7, 0.5, 0.3$, or 0.1, and with the velocity dispersion cut-off. Agreement between predictions and observations are obtained with $k_{\mathrm{fs}}(t_{\mathrm{eq}}) \approx 2\ \mathrm{Mpc}^{-1}$, and $0.8 \gtrsim n \gtrsim 0.3$.

$V_{\mathrm{flat}} \approx 45\ \mathrm{km/s}$. Similarly, for several masses M, the corresponding rotation velocities V_{flat} are summarized in **Table 3**. The data in **Table 3** can be fit by the relation

$$\frac{M}{M_{\odot}} \approx 2.1 \times 10^{8} \left(\frac{V_{\mathrm{flat}}}{10\ \mathrm{km/s}} \right)^{3}, \tag{5}$$

as shown in **Figure 6**. This becomes the Tully-Fisher relation, once $M/M_{\odot}$ is replaced by $\approx 10^{1.5}\, M_{*}/M_{\odot} \approx 10^{1.5}\, L_{*}/L_{\odot}$, see **Figure 1**.

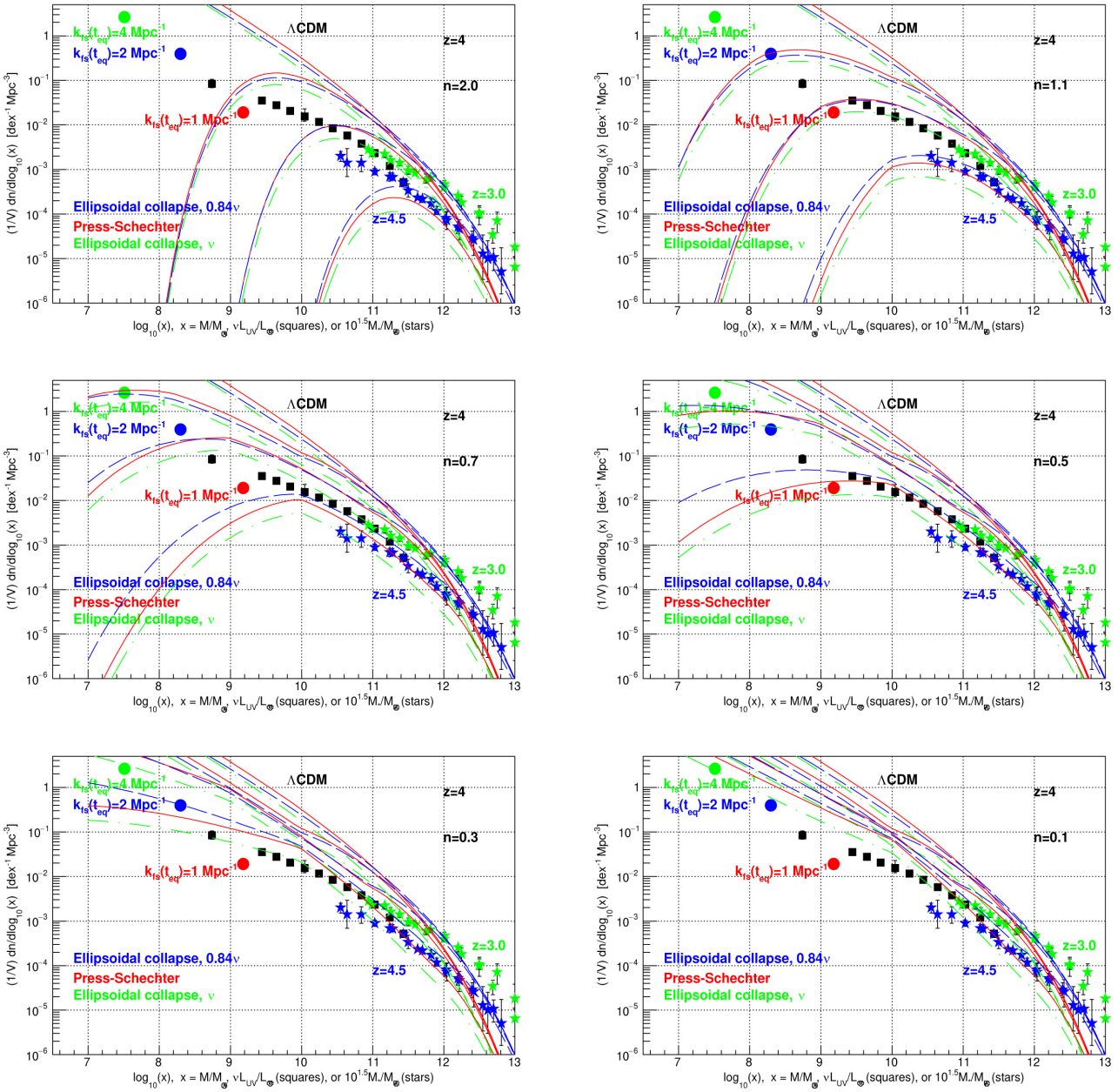

Figure 5. Predictions for $z = 4$, and (from top to bottom) $k_{\mathrm{fs}}(t_{\mathrm{eq}}) = 1000, 4, 2, 1\ \mathrm{Mpc}^{-1}$, are extended to $M < M_{\mathrm{vd0}}$ with the free-streaming cut-off with $\tau^2(k)$ with a tail with $n = 2.0, 1.1, 0.7, 0.5, 0.3$ or 0.1, and with the velocity dispersion cut-off. Agreement between predictions and observations are obtained with $k_{\mathrm{fs}}(t_{\mathrm{eq}}) \approx 1.5\ \mathrm{Mpc}^{-1}$ and $n \approx 0.7$, or $k_{\mathrm{fs}}(t_{\mathrm{eq}}) \approx 1\ \mathrm{Mpc}^{-1}$ and $n \approx 0.5$.

$$\frac{L_*}{L_\odot} \approx 2.4 \times 10^{10}\, h^{-2} \left(\frac{V_{\mathrm{flat}}}{200\ \mathrm{km/s}} \right)^3, \tag{6}$$

with $h = 0.674$. L_* is the stellar luminosity. The average bolometric luminosity of the sun is $M_\odot \equiv -2.5 \cdot \log_{10}\left(L_\odot / L_{\mathrm{ref}}\right) = 4.74$, so (6) becomes

$$M_{\mathrm{bol}} \approx -3.95 + 5 \cdot \log_{10}(h) - 7.5 \cdot \log_{10}\left(\frac{V_{\mathrm{flat}}}{\mathrm{km/s}} \right). \tag{7}$$

Table 2. The galaxy flat rotation velocity V_{flat} [km/s] is presented as a function of the adiabatic invariant $v_{h\text{rms}}(1)$, and the galaxy formation redshift z, for linear perturbations of total (dark matter plus baryon) mass $M = 2\times10^{10} M_{\odot}$. Also shown is the free-streaming cut-off wavenumber $k_{\text{fs}}(t_{\text{eq}})$ from (3). V_{flat} is obtained from numerical integration of galaxy formation hydro-dynamical equations [18].

$v_{h\text{rms}}(1)$ [m/s]	750	490	370	190	0.75
$k_{\text{fs}}(t_{\text{eq}})$ [Mpc^{-1}]	1	1.53	2	4	1000
z					
4	38	33	36	37	34
5	41	35	37	37	37
6	47	44	40	49	42
8	45	42	45	46	49
10	51	49	47	53	51

Table 3. Shown are linear perturbation total (dark matter plus baryon) masses M, and the corresponding flat rotation velocities V_{flat}. These relations are approximately valid for galaxy formation at redshift z between 6 and 10, and free-streaming cut-off wavenumber $k_{\text{fs}}(t_{\text{eq}})$ between 1 and 1000 Mpc^{-1}.

M	V_{flat}
$3\times10^{12} M_{\odot}$	255 km/s
$1\times10^{12} M_{\odot}$	188 km/s
$1\times10^{11} M_{\odot}$	82 km/s
$5\times10^{10} M_{\odot}$	71 km/s
$2\times10^{10} M_{\odot}$	45 km/s
$1\times10^{10} M_{\odot}$	37 km/s
$5\times10^{9} M_{\odot}$	28 km/s
$3\times10^{8} M_{\odot}$	9 km/s

This approximate relation, obtained from first principles, can be compared with the empirical Tully-Fisher relation (see **Figure 1** of [25] with $\Delta V \approx 3V_{\text{flat}}$).

5. The "Missing Satellites Problem"

The "Missing Satellites Problem" of the cold dark matter ΛCDM cosmology is described in [1]. The approximate number of observed satellites within $200h^{-1}$ kpc of the Local Group, per Mpc^3, with $V_{\text{flat}} > V$ is [1]

$$n_{\text{obs}}(V_{\text{flat}} > V) \approx 385h^3 \left(\frac{10 \text{ km/s}}{V}\right)^{1.3} \text{Mpc}^{-3}, \quad (8)$$

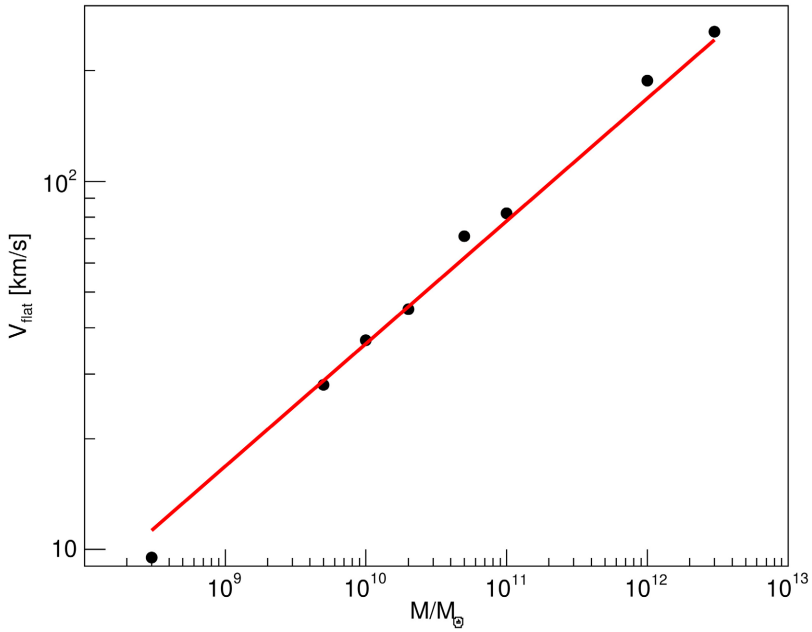

Figure 6. Presented is V_{flat}, from **Table 3**, as a function of the linear total (dark matter plus baryon) perturbation mass M, valid for galaxy formation at redshift z between 6 and 10, and free-streaming cut-off wavenumber $k_{\text{fs}}\left(t_{\text{eq}}\right)$ between 1 and 1000 Mpc^{-1}. The line is $M/M_{\odot} = 2.1\times 10^{8}\left(V_{\text{flat}}/10\text{ km/s}\right)^{3}$.

while the corresponding number in the ΛCDM simulations is [1]

$$n_{\text{sim}}\left(V_{\text{flat}} > V\right) \approx 5000h^{3}\left(\frac{10\text{ km/s}}{V}\right)^{2.75}\text{Mpc}^{-3}. \tag{9}$$

The difference between (8) and (9) illustrates the "Missing Satellites Problem" of the cold dark matter ΛCDM cosmology. The ratio of simulation to observation at each V_{flat} is

$$\frac{\mathrm{d}n_{\text{sim}}/\mathrm{d}V_{\text{flat}}}{\mathrm{d}n_{\text{obs}}/\mathrm{d}V_{\text{flat}}} \approx \frac{5000\times 2.75}{385\times 1.3}\left(\frac{10\text{ km/s}}{V_{\text{flat}}}\right)^{1.45}, \tag{10}$$

for satellites within $200h^{-1}$ kpc of the Local Group. Similarly, for satellites within $400h^{-1}$ kpc of the Local Group, the ratio is [1]

$$\frac{\mathrm{d}n_{\text{sim}}/\mathrm{d}V_{\text{flat}}}{\mathrm{d}n_{\text{obs}}/\mathrm{d}V_{\text{flat}}} \approx \frac{1200\times 2.75}{55\times 1.4}\left(\frac{10\text{ km/s}}{V_{\text{flat}}}\right)^{1.35}. \tag{11}$$

These ratios are approximately equal to 1 at $V_{\text{flat}} \approx 70$ km/s, corresponding to $M \approx 10^{10.9}M_{\odot}$, see (5). These ratios are approximately equal to 14 at $V_{\text{flat}} \approx 20$ km/s, corresponding to $M \approx 10^{9.2}M_{\odot}$, see (5).

Let us now consider the warm dark matter ΛWDM cosmology. We proceed as follows for each of the panels in **Figures 3-5**. We shift the ΛCDM prediction to the left until agreement with the data is obtained at $\log_{10}\left(x\right) = 10.9$, where x is $M/M_{\odot}$, or $10^{1.5}M_{*}/M_{\odot}$, or $\nu L_{\text{UV}}/L_{\odot}$. We then follow the shifted ΛCDM prediction to $\log_{10}\left(x\right) = 9.2$, and compare with the data. If the corresponding ratio

is in the approximate range 14 to 7 (to account for satellites found since the publication of [1]), and a good fit is obtained with $k_{\mathrm{fs}}\left(t_{\mathrm{eq}}\right)=2.0^{+0.8}_{-0.5}\ \mathrm{Mpc}^{-1}$ [6], we regard the parameter n of the prediction to be "good". If there is some tension, we clasify n as "fair". A summary is presented in **Table 4**. We conclude that for warm dark matter with $0.3\lesssim n\lesssim 0.8$, the predicted and observed number of satellites are in agreement, for galaxies formed with redshift $z\gtrsim 6$.

6. The UV Luminosity Cut-Off

Reionization begins in earnest at $z\approx 8$, and ends at $z\approx 6$. For each panel of **Figure 3**, corresponding to $z=8$, we integrate numerically the UV luminosity along the appropriate ellipsoidal collapse prediction (with parameter 0.84ν), that obtains excellent agreement with the data. The following procedure is followed in [4]: the observed UV luminosity distribution is extended (without the Δz velocity dispersion cut-off) to an assumed sharp UV magnitude cut-off M_{UV}, and the corresponding reionization optical depth τ is calculated. Here we obtain the equivalent sharp UV magnitude cut-off M_{UV}, and then the corresponding reionization optical depth τ from [4]. The results are summarized in **Table 5**. We note that, for the range $0.5\lesssim n\lesssim 0.8$, we obtain agreement with the measured reionization optical depth $\tau=0.053\pm 0.007$ obtained by the Planck collaboration [2] [3].

Table 4. Values of the non-linear small scale regeneration parameter n that obtain "good", "fair", or "poor" agreement with the "Missing Satellites Problem", as a function of the redshift of galaxy formation z, obtained from the panels in **Figures 3-5**.

Redshift z	Good	Fair	Poor
8	0.3, 0.5, 0.7		0.1, 1.1, 2.0
6	0.3, 0.5, 0.7		0.1, 1.1, 2.0
4		0.7	0.1, 0.3, 0.5, 1.1, 2.0

Table 5. For $z=8$ and each n we obtain the equivalent sharp UV magnitude cut-off M_{UV}, and then the corresponding reionization optical depth τ from [4]. For comparison, the Planck collaboration measurement is $\tau=0.053\pm 0.007$ [2] [3].

n	M_{UV}	τ	fit quality
0.9	−18.6	0.050 ± 0.006	fair
0.8	−18.3	0.050 ± 0.006	good
0.7	−17.6	0.052 ± 0.006	excellent
0.6	−16.9	0.053 ± 0.008	excellent
0.5	−14.9	0.059 ± 0.008	excellent
0.4	>−11.9	>0.07	good
0.3	>−11.9	>0.07	fair

7. Conclusions

Comparisons of the rest frame galaxy UV luminosity distributions, and galaxy stellar mass distributions, with predictions for $M > M_{\mathrm{vd}}$, obtain the free-streaming cut-off wavenumber $k_{\mathrm{fs}}\left(t_{\mathrm{eq}}\right) = 2.0^{+0.8}_{-0.5}\ \mathrm{Mpc}^{-1}$, with the non-linear regeneration of small scale structure parameter n in the wide approximate range 0.2 to 1.1 [6]. In the present work we have extended the predictions of the warm dark matter ΛWDM cosmology to $M < M_{\mathrm{vd}}$, including the free-streaming cut-off (4), and the velocity dispersion cut-off of **Table 2**. This extension is in agreement with the number of satellites of galaxies formed at $z \gtrsim 6$, and with the needed UV cut-off (to not exceed the observed reionization optical depth), with n in the approximate range 0.5 to 0.8.

As a cross-check, we have obtained the adiabatic invariant in the core of dwarf galaxies dominated by dark matter, from their rotation curves. The result is $v_{\hbar\mathrm{rms}}(1) = 0.406 \pm 0.069\ \mathrm{km/s}$ [21], corresponding to a free-streaming cut-off wavenumber $k_{\mathrm{fs}}\left(t_{\mathrm{eq}}\right) = 1.90 \pm 0.32\ \mathrm{Mpc}^{-1}$, from Equation (1). This result confirms: 1) that the adiabatic invariant in the core of galaxies is of cosmological origin, as predicted for warm dark matter [18], since several galaxies accurately share the same adiabatic invariant, and 2) confirms that $k_{\mathrm{fs}}\left(t_{\mathrm{eq}}\right)$ is due to free-streaming. All of these results are data driven.

As a by-product of this study we obtain approximately the empirical Tully-Fisher relation from first principles, by integrating numerically the galaxy formation hydro-dynamical equations [18]. These hydro-dynamical equations predict that the core of first galaxies form adiabatically if dark matter is warm, *i.e.* conserves $v_{\hbar\mathrm{rms}}(1)$.

Omitting the non-linear regeneration of small scale structure, *i.e.* setting $n = 2$, or using the similar $\tau^2(k)$ from the linear Equation (7) of [26], and omitting the velocity dispersion cut-off, obtains strong disagreement with observations. These omissions have led several published studies to obtain lower warm dark matter particle "thermal relic mass" limits of several keV. Note that nature, and simulations [23], re-generate non-linear small scale structure when relative density perturbations approach unity. May I suggest that these mass limits be revised, including the non-linear regeneration of small scale structure, and the velocity dispersion cut-off. We note that the Particle Data Group's "Review of Particle Physics (2022)" quotes lower limits of 70 eV for fermion dark matter, or 10^{-22} eV for bosons [3], not several keV.

To summarize, warm dark matter with an adiabatic invariant $v_{\hbar\mathrm{rms}}(1) = 0.406 \pm 0.069\ \mathrm{km/s}$ [21], a free-streaming comoving cut-off wavenumber $k_{\mathrm{fs}}\left(t_{\mathrm{eq}}\right) = 2.0^{+0.8}_{-0.5}\ \mathrm{Mpc}^{-1}$ [6], and a non-linear small scale regenerated "tail" as in (4) with $0.5 \lesssim n \lesssim 0.8$, is in agreement with galaxy rotation curves [21], galaxy stellar mass distributions, galaxy rest frame UV luminosity distributions [6], the Missing Satellites Problem, and the UV luminosity cut-off needed to not exceed the measured reionization optical depth.

Conflicts of Interest

The author declares no conflicts of interest regarding the publication of this paper.

References

[1] Klypin, A.A., Kravstov, A.V. and Valenzuela, O. (1999) Where Are the Missing Galactic Satellites? *The Astrophysical Journal*, **522**, 82-92. https://doi.org/10.1086/307643

[2] Aghanim, N., *et al.* (2018) Planck 2018 Results. VI. Cosmological Parameters. *Astronomy & Astrophysics*, **641**, A6.

[3] Workman, R.L., *et al.* (Particle Data Group) (2022) The Review of Particle Physics. *Progress of Theoretical and Experimental Physics*, **2022**, 083C01.

[4] Lapi, A. and Danese, L. (2015) Cold or Warm? Constraining Dark Matter with Primeval Galaxies and Cosmic Reionization after Planck. *Journal of Cosmology and Astroparticle Physics*, **9**, 3. https://doi.org/10.1088/1475-7516/2015/09/003

[5] Mason, C.A., Trenti, M. and Treu, T. (2015) The Galaxy UV Luminosity Function before the Epoch of Reionization. *The Astrophysical Journal*, **813**, 21. https://doi.org/10.1088/0004-637X/813/1/21

[6] Hoeneisen, B. (2022) Measurement of the Dark Matter Velocity Dispersion with Galaxy Stellar Masses, UV Luminosities, and Reionization. *International Journal of Astronomy and Astrophysics*, **12**, 258-272. https://doi.org/10.4236/ijaa.2022.123015

[7] Press, W.H. and Schechter, P. (1974) Formation of Galaxies and Clusters of Galaxies by Self-Similar Gravitational Condensation. *The Astrophysical Journal*, **187**, 425-438. https://doi.org/10.1086/152650

[8] Sheth, R.K. and Tormen, G. (1999) Large-Scale Bias and the Peak Background Split. *Monthly Notices of the Royal Astronomical Society*, **308**, 119-126. https://doi.org/10.1046/j.1365-8711.1999.02692.x

[9] Sheth, R.K., Mo, H.J. and Tormen, G. (2001) Ellipsoidal Collapse and an Improved Model for the Number and Spatial Distribution of Dark Matter Haloes. *Monthly Notices of the Royal Astronomical Society*, **323**, 1-12. https://doi.org/10.1046/j.1365-8711.2001.04006.x

[10] Lapi, A., *et al.* (2017) Stellar Mass Function of Active and Quiescent Galaxies via the Continuity Equation. *The Astrophysical Journal*, **847**, 13. https://doi.org/10.3847/1538-4357/aa88c9

[11] Song, M., Finkelstein, S.L., Ashby, M.L.N., *et al.* (2016) The Evolution of the Galaxy Stellar Mass Function at $z = 4$-8: A Steepening Low-Mass-End Slope with Increasing Redshift. *The Astrophysical Journal*, **825**, 5. https://doi.org/10.3847/0004-637X/825/1/5

[12] Grazian, A., Fontana, A., Santini, P., *et al.* (2015) The Galaxy Stellar Mass Function at $3.5 \leq z \leq 7.5$ in the CANDELS/UDS, GOODS-South, and HUDF Fields. *Astronomy and Astrophysics*, **575**, A96. https://doi.org/10.1051/0004-6361/201424750

[13] Davidzon, I., Ilbert, O., Laigle, C., *et al.* (2017) The COSMOS2015 Galaxy Stellar Mass Function: 13 Billion Years of Stellar Mass Assembly in 10 Snapshots. *Astronomy and Astrophysics*, **605**, A70. https://doi.org/10.1051/0004-6361/201730419

[14] Bouwens, R.J., *et al.* (2015) UV Luminosity Functions at Redshifts $z \approx 4$ to $z \approx 10$: 10000 Galaxies from HST Legacy Fields. *The Astrophysical Journal*, **803**, 34. https://doi.org/10.1088/0004-637X/803/1/34

[15] Bouwens, R.J., *et al.* (2021) New Determinations of the UV Luminosity Functions from z ≈ 9 to z ≈ 2 Show a Remarkable Consistency with Halo Growth and a Constant Star Formation Efficiency. *The Astronomical Journal*, **162**, 47. https://doi.org/10.3847/1538-3881/abf83e

[16] McLeod, D.J., *et al.* (2015) New Redshift z ≈ 9 Galaxies in the Hubble Frontier Fields: Implications for Early Evolution of the UV Luminosity Density. *MNRAS*, **450**, 3032. https://doi.org/10.1093/mnras/stv780

[17] Bouwens, R.J., Illingworth, G.D. and Oesch, P.A. (2014) UV-Continuum Slopes of 4000 $z \approx$ 4-8 Galaxies from the HUDF/XDF, HUDF09, ERS, CANDELS-South, and CANDELS-Northfields. *The Astrophysical Journal*, **793**, 115. https://doi.org/10.1088/0004-637X/793/2/115

[18] Hoeneisen, B. (2022) Warm Dark Matter and the Formation of First Galaxies. *Journal of Modern Physics*, **13**, 932-948. https://doi.org/10.4236/jmp.2022.136053

[19] Paduroiu, S., Revaz, Y. and Pfenniger, D. (2015) Structure Formation in Warm Dark Matter Cosmologies Top-Bottom Upside-Down. *Monthly Notices of the Royal Astronomical Society*. https://arxiv.org/pdf/1506.03789.pdf

[20] Hoeneisen, B. (2022) Comments on Warm Dark Matter Measurements and Limits. *International Journal of Astronomy and Astrophysics*, **12**, 94-109. https://doi.org/10.4236/ijaa.2022.121006

[21] Hoeneisen, B. (2022) Measurement of the Dark Matter Velocity Dispersion with Dwarf Galaxy Rotation Curves. *International Journal of Astronomy and Astrophysics*, **12**, 363-381. https://doi.org/10.4236/ijaa.2022.124021

[22] Boyanovsky, D., de Vega, H.J. and Sanchez, N.G. (2008) The Dark Matter Transfer Function: Free Streaming, Particle Statistics and Memory of Gravitational Clustering. *Physical Review D*, **78**, Article ID: 063546. https://doi.org/10.1103/PhysRevD.78.063546

[23] White, M. and Croft, R.A.C. (2018) Suppressing Linear Power on Dwarf Galaxy Halo Scales. *The Astrophysical Journal*, **539**, 497-504. https://doi.org/10.1086/309273

[24] Weinberg, S. (2008) Cosmology. Oxford University Press, Oxford.

[25] Tully, R.B. and Fisher, J.R. (1977) A New Method of Determining Distances to Galaxies. *Astronomy and Astrophysics*, **54**, 661-673.

[26] Markovič and Viel, M. (2013) Lyman-α Forest and Cosmic Weak Lensing in a Warm Dark Matter Universe. Cambridge University Press, Cambridge. https://doi.org/10.1017/pasa.2013.43